Old puzzle of incommensurate crystal structure of calaverite $AuTe_2$ and predicted stability of novel AuTe compound

Sergey V. Streltsov[a,b,1], Valerii V. Roizen[c], Alexey V. Ushakov[a], Artem R. Oganov[c,d], and Daniel I. Khomskii[e]

[a]Department of Theory of Low-Dimensional Spin Systems, Institute of Metal Physics, 620990 Yekaterinburg, Russia; [b]Department of Theoretical Physics and Applied Mathematics, Ural Federal University, 620002 Yekaterinburg, Russia; [c]Computational Materials Discovery Laboratory, Moscow Institute of Physics and Technology, 141701 Dolgoprudny, Moscow Region, Russian Federation; [d]Materials Discovery Laboratory, Skolkovo Institute of Science and Technology, 143026 Skolkovo, Russian Federation; and [e]II. Physikalisches Institut, Universität zu Köln, D-50937 Cologne, Germany

Edited by James R. Chelikowsky, The University of Texas at Austin, Austin, Texas, and accepted by Editorial Board Member John D. Weeks August 14, 2018 (received for review February 15, 2018)

Gold is a very inert element, which forms relatively few compounds. Among them is a unique material—mineral calaverite, $AuTe_2$. Besides being the only compound in nature from which one can extract gold on an industrial scale, it is a rare example of a natural mineral with incommensurate crystal structure. Moreover, it is one of few systems based on Au, which become superconducting (at elevated pressure or doped by Pd and Pt). Using ab initio calculations we theoretically explain these unusual phenomena in the picture of negative charge-transfer energy and self-doping, with holes being largely in the Te 5*p* bands. This scenario naturally explains incommensurate crystal structure of $AuTe_2$, and it also suggests a possible mechanism of superconductivity. An ab initio evolutionary search for stable compounds in the Au–Te system confirms stability of $AuTe_2$ and $AuTe_3$ and leads to a prediction of an as yet unknown stable compound AuTe, which until now has not been synthesized.

incommensurate crystal structure | calaverite | superconductivity

It is very well known that gold is one of the least reactive chemical elements and it is typically mined as a pure native element. It also occurs in alloys but very rarely it can be found in the form of compounds. The only compound existing in nature from which one can extract gold on an industrial scale is gold telluride—$AuTe_2$, calaverite. This material is extremely interesting in many aspects. It even influenced the gold rush in Australia, where miners in gold mines first discarded calaverite as an "empty" waste and used it for paving the roads, but, after discovering that it contains real gold which can be extracted, very carefully scrapped all these roads.

Another, very specific feature of $AuTe_2$ is that it is one of very few materials having in natural form an incommensurate crystal structure. This at one time was of much concern to mineralogists and crystallographers: They could not understand the peculiar faceting of calaverite crystals, contradicting Haüy's law. Usually the stable natural facets of a crystal are those with small Miller indexes, and in calaverite everything looked odd, until it was realized that the very crystal structure is incommensurate (1). But the origin of the incommensurability is still obscure. Last but not least, $AuTe_2$ was found to be a superconductor at a relatively low pressure of 2.3 GPa or upon Pt or Pd doping (2–5), with critical temperature ~ 4 K.

In the present paper, we show that all these properties of $AuTe_2$ can be naturally explained, if one takes into account that it is in a negative charge-transfer energy regime, which drives a charge disproportionation resulting in an incommensurate crystal structure at normal conditions or a superconducting state at higher pressures. Moreover, an extensive structural study of different gold tellurides allowed us to predict the existence of a hitherto unknown compound: AuTe. We report the predicted crystal structure and properties of this material.

Old Puzzle of Calaverite's Crystal Structure

$AuTe_2$ has a distorted layered CdI_2-type structure [the average structure has space group $C2/m$ (6)], with triangular layers of Au with Te atoms in between. However, there is a periodic displacive modulation along the [010] direction, which makes overall crystal structure incommensurate (7). The mechanism of incommensurability is unclear. One may argue that it can be due to a specific electronic structure, which results in a charge density wave (CDW) instability, but accurate band structure calculations have not found nesting of the Fermi surface at corresponding wave vectors (8, 9). Schutte and de Boer (10) proposed another explanation based on the formal assignment of valencies in $Au^{2+}(Te_2)^{2-}$ [in analogy with another mineral—the "fool's gold" $Fe^{2+}(S_2)^{2-}$]. However, whereas Fe^{2+} is a stable ionic state, every chemist knows that Au^{2+} is extremely difficult to stabilize: It exists as $Au^{1+}(d^{10})$ or Au^{3+} (nominally low-spin d^8). If one could manage to really stabilize $Au^{2+}(d^9)$, it would be a realization of an old dream—a "magnetic gold." [It was actually indeed made, however not in oxides, but in systems with more ionic bonds—in $Au(AuF_4)_2$ and $Au(SbF_6)_2$ (11).]

The phenomenon of skipped valence (12) of Au^{2+} can lead to the possibility of charge disproportionation into Au^{1+} and Au^{3+}, and it seems to naturally explain the ground-state properties of $AuTe_2$, as it works for example in $Cs_2Au_2Cl_6$ (13).

Significance

It is shown that the long-standing puzzle of incommensurate crystal structure of $AuTe_2$ can be solved, if this material is considered as a negative charge-transfer system. Using modern computational methods, we demonstrate that charge redistribution associated with incommensurate modulations of crystal structure occurs not so much on Au, but predominantly on Te sites. This substantially reduces Coulomb energy costs for creating such a unique crystal structure. The same mechanism also explains superconductivity of doped $AuTe_2$. Exploring different Au–Te compositions, we also discovered a previously unknown compound AuTe, which theoretically is very stable, and we predict its crystal structure.

Author contributions: S.V.S. and D.I.K. designed research; S.V.S., V.V.R., and A.V.U. performed calculations; S.V.S., A.R.O., and D.I.K. analyzed data; and S.V.S. and D.I.K. wrote the paper.

The authors declare no conflict of interest.

This article is a PNAS Direct Submission. J.R.C. is a guest editor invited by the Editorial Board.

[1]To whom correspondence should be addressed. Email: streltsov.s@gmail.com.

This article contains supporting information online at www.pnas.org/lookup/suppl/doi:10.1073/pnas.1802836115/-/DCSupplemental.

Published online September 19, 2018.

The fact that the CDW due to such charge disproportionation is incommensurate in $AuTe_2$, in contrast to $Cs_2Au_2Cl_6$, may be related to the triangular lattice, which Au ions form in $AuTe_2$. This lattice is not bipartite, and the resulting frustration can lead to incommensurate modulation. While overall modulation of the lattice is complex, the local distortions seem to confirm this skipped valence interpretation: Some Au ions, say at the maximum of CDW, are in a linear, or dumbbell coordination (two short and four long Au–Te bonds), typical for d^{10} ions, here Au^{1+}, whereas at the "other end," say in the minimum of the CDW, Au ions are square coordinated—coordination typical for $Au^{3+}(t_{2g}^6(3z^2-r^2)^2(x^2-y^2)^0)$ (5). Local surroundings for other Au interpolate between these two limits.

This interpretation, however, was put in doubt. First, photoemission (14) and then X-ray absorption (15) measurements showed that apparently electronic configuration of all Au ions is the same, close to Au^{1+}. [A recent spectroscopic study, however, did show the existence of slightly inequivalent Au ions (4).] Also ab initio calculations performed for the artificial supercell structure with four Au ions mimicking the small-period CDW do not show any difference in occupation of the d shell for different Au ions (8). (Note that the structure used in ref. 8 is somehow unnatural in a sense that four short Au–Te bonds do not lie in one plane.)

We argue that nevertheless the physics of $AuTe_2$ is related to the eventual instability of Au^{2+} against charge disproportionation, which determines the main properties of $AuTe_2$, including not only incommensurate CDW, but also the tendency to superconductivity. As demonstrated below, the resolution of the controversy mentioned above lies in the fact that actually $AuTe_2$ is a negative charge-transfer (CT) energy system (16, 17), with all of the holes predominantly in the $5p$ bands of Te.

The notion of CT insulators was introduced in the seminal paper by Zaanen, Sawatzky, and Allen (18). These are materials with strongly correlated electrons. However, the lowest charge excitations in them correspond not to transfer of electrons between localized d states, $d^n d^n \rightarrow d^{n+1} d^{n-1}$, as in Mott–Hubbard insulators, but to electron transfer between ions of transition metals (TMs) and ligands, that is, to the processes $d^n p^6 \rightarrow d^{n+1} p^5 = d^{n+1}\underline{L}$, where $\underline{L}$ stands for the ligand hole. In CT insulators this CT excitation energy is positive, $\Delta_{CT} = E(d^{n+1}p^5) - E(d^n p^6) > 0$, but in principle it can be very small or even negative (naively speaking, when anion p levels lie above d levels of TM ions). In this case we refer to negative CT energy. Usually this situation is met when the oxidation state of a metal is unusually high—e.g., 4+ for Fe or 3+ for Cu. If such states are created by doping, as in high-T_c cuprates, the doped holes go predominantly to oxygen p states (although these are of course strongly hybridized with d states of Cu). But this situation can be realized also in undoped stoichiometric compounds such as $CaFeO_3$. In this case there can occur spontaneous transfer of electrons from ligands to the TM ion, that is, $Fe^{4+} \rightarrow Fe^{3+}\underline{L}$. This situation can be called a self-doping (19). This picture, which in physics we describe by the (negative) CT energy, is reminiscent of the notion of dative bonding in chemistry [A "dictionary" helping to establish the correspondence between physical and chemical language is contained in the famous book by Goodenough (20) and a very clear paper by Hoffmann et al. (21).]

Interestingly enough, in many systems of this class there occurs spontaneous charge disproportionation, like $2Fe^{4+} \rightarrow Fe^{3+}+Fe^{5+}$, but occurring predominantly on ligands; that is, this "reaction" should be visualized as $2Fe^{3+}\underline{L} \rightarrow Fe^{3+}+Fe^{3+}\underline{L}^2$. This process is now well established also in nickelates $RNiO_3$ (R = Pr, Nd), where it leads to a real phase transition, originally interpreted as charge ordering on Ni ($2Ni^{3+} \rightarrow Ni^{2+} + Ni^{4+}$) (22), but which is actually much better described by the reaction $2Ni^{2+}\underline{L} \rightarrow Ni^{2+} + Ni^{1+}\underline{L}^2$ (23).

We claim that the same phenomenon also occurs in systems containing Au^{2+}, such as, e.g., $Cs_2Au_2Cl_6$ (13), and also in calaverite $AuTe_2$, where one can write this reaction as

$$2Au^{2+}(d^9) \rightarrow Au^{1+}(d^{10}) + Au^{3+}(d^8), \quad [1]$$

but in fact it should be visualized as

$$2Au^{2+} \equiv 2Au^{1+}\underline{L} \rightarrow Au^{1+} + Au^{1+}\underline{L}^2. \quad [2]$$

Two holes ($\underline{L}^2$) in the Te p band form something like a bound state, with the symmetry of a low-spin d^8 state of Au^{3+} with which it hybridizes. Below we confirm this picture by the ab initio band structure calculations.

Mechanism of Incommensurability in $AuTe_2$: Negative CT Gap Energy

It is impossible to carry out ab initio calculations for the real incommensurate structure with the existing codes based on density function theory (DFT). One needs to approximate this structure by some supercell with a commensurate CDW. We borrowed an idea on how to construct it from nature, taking the initial crystal structure from the mineral sylvanite—$AuAgTe_4$. Au and Ag ions in sylvanite are ordered in stripes, with Ag being in a linearly coordinated site, typical for ions with d^{10} configuration, that is, it is Ag^{1+} (Au-D in Fig. 1*B*); and Au ions occupy a square-coordinated position, corresponding to, nominally, Au^{3+} (Au-P in Fig. 1*B*) with its strong Jahn–Teller distortion (6). This structure was relaxed in the generalized gradient approximation (GGA), taking into account the spin–orbit coupling (SOC), and then Ag was substituted by an Au ion and relaxed again, keeping the unit cell volume the same as in real $AuTe_2$ (this structure is labeled as AuAu'Te_4 in what follows).

First, we found that the AuAu'Te_4 structure is stable and there are still two differently coordinated Au ions. Second, this structure is lower in energy than the average $C2/m$ structure (6) at experimental volume [by 22 meV/formula units (f.u.)]. Thus, one may see that we gain a lot of energy by making distortions corresponding to the CDW (in this case a commensurate one).

A close inspection of the Au $5d$ occupation numbers in the AuAu'Te_4 structure, however, shows that from the point of view of d occupation both Au ions are 1+: Corresponding occupancies of the d shell [as obtained within the projector augmented wave (PAW) method] are 9.90 and 9.92, so that the difference is negligible: $\delta n_{Au-d} = 0.02$ electrons [the Bader analysis (24) gives an even smaller difference, <0.01 electrons] (note that in real sylvanite, $AuAgTe_4$, $\delta n \sim 0.5$ electrons; that is, in sylvanite we can indeed refer to Ag^{1+} and Au^{3+}, Au^{3+} again with a lot

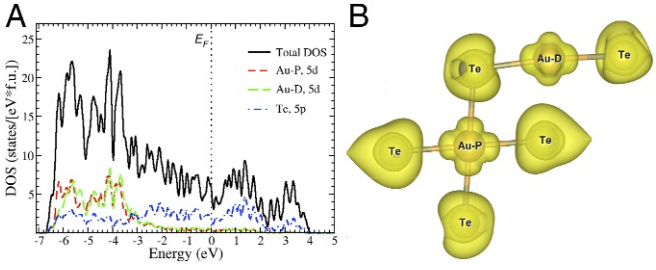

Fig. 1. (*A*) GGA + SOC total and partial density of states for the AuAu'Te_4 structure (for experimental volume). (*B*) Charge density $\rho(\vec{r})$ corresponding to the topmost, partially filled band [isosurface corresponding to 0.003 $e/Å^3 \approx 10\%$ of maximal value of $\rho(\vec{r})$ is presented. Shown are results of the GGA + SOC calculations for $AuTe_2$ in the fully optimized "$AuAgTe_4$" structure. Au-P and Au-D stand for Au ions having plaquette and dumbbell surroundings.

of ligand holes). This, however, seems to be in strong contrast with results from the lattice optimization, which give very different local coordination for two Au ions: We have one linearly coordinated (1+) and another square-coordinated (3+) Au. The difference between short and long Au–Te bonds is ∼0.25 Å in linear-coordinated and ∼0.35 Å in square-coordinated Au. This is of the order of magnitude of Jahn–Teller (JT) distortions in such classical JT systems as $LaMnO_3$ (0.27 Å) (25) and K_2CuF_4 (∼0.3 Å) (26). What drives such strong lattice distortions, if not the CDW on Au sites?

To answer this question we plot in Fig. 1*B* the distribution of the charge density corresponding to the topmost, partially filled bands illustrating a hole distribution. One may see that there is only a minor contribution from the Au $5d$ states to the charge density corresponding to the least-filled band, while the largest part comes from the Te $5p$ orbitals. Thus, one may note a significant contribution of the ligand holes to the ground-state wave function. The symmetry of the ($\underline{L}^2$) hole state around "Au^{3+}" (Au-P in Fig. 1*B*) is the same as that of a hypothetical JT active Au^{3+} ion with two holes on the x^2-y^2 orbital; that is, it naturally explains why this ion has square coordination typical for such a state. (Note that this orbital lies in the plane of the Te plaquette, while the central part of the charge density at Au-D is spherically symmetric and, thus, this band corresponds instead to the $3z^2-r^2$ orbital.)

Analysis of the density of states, shown in Fig. 1*A*, also confirms that the largest number of holes are in the Te $5p$ bands and one may note a negative CT energy situation. The local electronic structure of Au ions in this case corresponds to 1+ valence state for all Au ions (d^{10}). These results allow us to reconcile the picture of charge disproportionation driven largely by skipped valence of Au^{2+} with the experimental data (14, 15), which show that all Au ions are Au^{1+} from the spectroscopic point of view.

Moreover, a redistribution of electrons between Te and Au favors a strongly distorted calaverite crystal structure, reminiscent of the formation of the CDW. Indeed, if the CT energy were positive and there were a real CDW with the Au^{1+} and Au^{3+} ions having $5d^{10}$ and $5d^8$ electronic configurations, this would cost a lot of Coulomb energy (two holes on the same d site repel each other with the energy U, which is ∼10 eV). Redistributing a part of the charge density to ligands, we minimize the energy costs of the formation of the CDW.

However, analysis of only two structures can be only qualitative. There is no guarantee that there are no other structures, which would give a lower total energy. In addition, the equilibrium volume in the DFT can be different from that in the experiment. To overcome the first difficulty we used the evolutionary algorithm USPEX (27) to search for all possible structures of $AuTe_2$ with all experimentally known structures included in the calculation. USPEX was previously successfully applied for investigation of structural properties of many different materials, including those based on heavy metals (28–30). For $AuTe_2$ we found that the AuAu'Te_4 structure with distortions resembling the CDW still has the lowest total energy among hundreds of other structures obtained with the USPEX. There appear to be only two structures (in the interval of 100 meV per atom) which may compete with it: the high-pressure $P\bar{3}m1$ phase, where the incommensurate superstructure disappears and all Au ions become structurally equivalent, and a structure characterized by the $Cmmm$ space group, the total energy of which is by 90 meV per atom higher than that of AuAu'Te_4.

In the second step we carefully checked how total energies of these crystal structures depend on the volume (Fig. 2). The AuAu'Te_4 structure corresponding to the CDW is still the lowest one, while the equilibrium volume is slightly overestimated. The next one is $P\bar{3}m1$ with 5.5% smaller volume, and the average $C2/m$ and $Cmmm$ structures are much higher in energy.

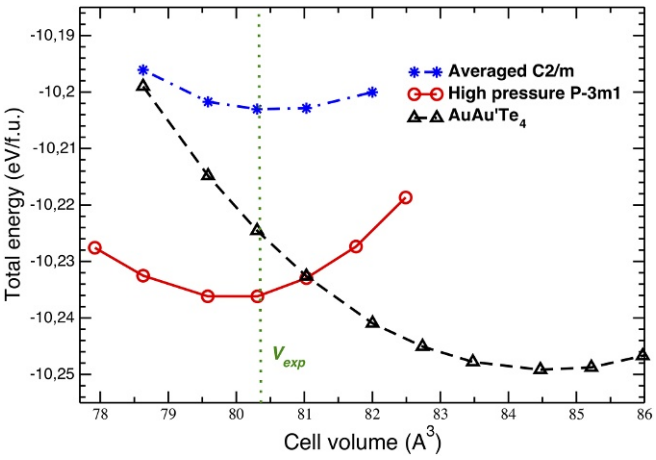

Fig. 2. Total energy vs. volume for different possible crystal structures (GGA + SOC results). For each volume, optimization of the crystal structure was performed.

At this stage one can demonstrate a crucial role of the CT energy for the formation of the AuAu'Te_4 structure with distortions, imitating the real structure of $AuTe_2$. For this we performed model calculations, where the Au $5d$ bands were artificially shifted up in energy, thus increasing the CT energy and reducing the contribution of Te holes. We found that the shift of only 1 eV is enough to destabilize the AuAu'Te_4 structure, and it makes the high-pressure $P\bar{3}m1$ phase with all Au ions structurally equivalent the lowest in energy: The total energy difference is $E_{P\bar{3}m1}-E_{\mathrm{AuAu'Te_4}}\approx -2$ meV/f.u. In the real $AuTe_2$, modeled by AuAu'Te_4, the Au $5d$ states lie below Te $5p$ (Fig. 1*A*), which corresponds to a negative CT energy Δ_{CT}. Shifting the Au $5d$ orbitals up leads to a decrease of absolute value of Δ_{CT} or even can make it positive. Then the charge disproportionation would have been mostly on the Au sites, which leads to a drastic increase of the energy costs of the CDW due to Coulomb interaction, as explained above, and as a result the AuAu'Te_4 structure with inequivalent Aus becomes much higher in energy.

An important question is why in real $AuTe_2$ the superstructure is incommensurate. As explained above, due to computational limitations we had to model it by the closest commensurate structure of a sylvanite, our AuAu'Te_4. To check for the possibility to get incommensurate structure we calculated the phonon spectrum (31) of $AuTe_2$. We indeed found that when we start from the homogeneous high-pressure phase $P\bar{3}m1$, some phonon frequencies became imaginary with the minimal frequency at incommensurate wave vectors $\mathbf{q}\approx 0.41\mathbf{a}+0.5\mathbf{c}$ (where **a** and **c** correspond to the $P\bar{3}m1$ structure) (*SI Appendix*, Fig. S1*B*). Thus, the real instability of the homogeneous structure would indeed lead to an incommensurate superstructure.

Very significantly, when we shift d levels up, as explained above, these imaginary phonon frequencies disappear. This once again proves that the negative CT energy and corresponding large contribution of ligand holes are crucial for the formation of the incommensurate structure of $AuTe_2$.

High-Pressure Phase and Superconductivity

Taking the first derivative of $E(V)$, one can find that a critical pressure (P_c) required for the transition from AuAu'Te_4 to $P\bar{3}m1$ is 2.6 GPa. It is striking that while our optimized structure with the commensurate CDW (AuAu'Te_4) slightly overestimates equilibrium volume, the critical pressure for the transition to uniform $P\bar{3}m1$ is reproduced with good accuracy: The experimental $P_c=2.5$ GPa (5).

PHYSICS

The high-pressure phase of $AuTe_2$ is also very interesting due to another aspect—the superconductivity, which appears in it below $T_c = 2.3$ K (2). One may stabilize this phase not only by pressure, but also by Pt doping (3), which also results in the stabilization of the same $P\bar{3}m1$ structure. The superconductivity was proposed to be induced by breaking of Te–Te dimers, which exist in the $C2/m$ phase, but disappear in the high-pressure superconducting $P\bar{3}m1$ phase (3). In particular, it was speculated that the formation of Te–Te dimers modifies the electronic structure of $AuTe_2$ through formation of bonding (σ) and antibonding (σ^*) Te $5p$ bands (3). We have seen that the bands at the Fermi level indeed have a very large contribution of the Te $5p$ states, but they are strongly hybridized with Au $5d$ and have the symmetry of Au $5d$ orbitals (Fig. 1), while the σ-bonded Te $5p$ states are far away from the Fermi level ($\sim$5.2 eV below and $\sim$3.2 eV above E_F). Thus, it seems that the Te–Te dimerization is not directly related to the suppression of the superconductivity. In fact, this is just one of the consequences of the formation of the CDW. In Fig. 3 the directions of Te atom displacements due to the CDW are indicated. One may see that the formation of $AuTe_4$ plaquettes and $AuTe_2$ dumbbells naturally results in dimerization of the Te atoms, which, however, is not a driving force but rather a consequence of the CDW formation in $AuTe_2$.

One can argue that the physics disclosed in our calculations, specifically the origin of the incommensurability—the tendency to the skipped valence and charge disproportionation of "Au^{2+}," occurring in the situation with negative CT energy with the self-doping—is also instrumental in providing a mechanism of superconductivity in $AuTe_2$ under pressure or with doping. This tendency, both on the d levels (reaction Eq. **1**) and more realistically on ligand states (reaction Eq. **2**), means that there exists a tendency for holes to form pairs; that is, there exists an effective attraction of these holes.

The idea that the tendency to charge disproportionation (which actually means the local "chemical" tendency to form pairs of electrons or holes) can be instrumental in providing the mechanism of Cooper pairing was first suggested by Rice and Sneddon (32) in connection with the superconductivity of doped $BaBiO_3$. This material is also known to experience charge disproportionation of the type $2Bi^{4+} \rightarrow Bi^{3+} + Bi^{5+}$ (and again with a lot of action on ligands, e.g., ref. 17). For high-T_c cuprates a similar idea was proposed in ref. 33. It is also closely related to some theoretical studies of superconductivity in systems with coexisting ordinary electrons and bipolarons (e.g., refs. 34 and 35). We suppose, by analogy with the abovementioned papers,

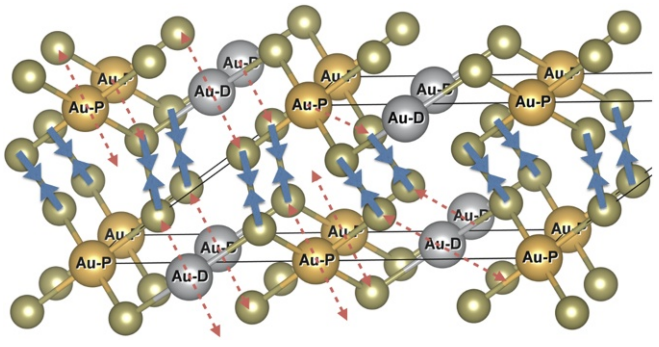

Fig. 3. Formation of the Te–Te dimers due to charge disproportionation on Au sites. The "strength" of distortions in $AuTe_6$ octahedra is not the same for all Au–Te bonds. There are "strongly" distorted with respect to undistorted $P\bar{3}m1$ ($\delta_{Au-Te} \sim 0.45 - 0.55$ Å) and "weakly" distorted Au–Te bonds ($\delta_{Au-Te} \sim 0.15$ Å). Plotting (for simplicity) only strongly distorted Au–Te bonds (red lines; arrows show direction of distortions), one immediately obtains Te–Te dimers (shown by blue arrows).

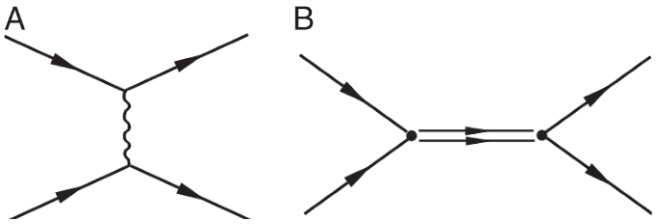

Fig. 4. (*A* and *B*) Diagrams illustrating (*A*) conventional Bardin–Cooper–Schrieffer "t-channel" pairing and (*B*) "s-channel" pairing proposed for $AuTe_2$.

that the chemical tendency of Au^{2+} to charge disproportionately into, nominally, Au^{1+} and Au^{3+}, which is the main ingredient of our theory and which, as we argued above, plays a crucial role in explaining the main properties of $AuTe_2$, may be also instrumental in providing the mechanism, or at least helping the realization, of superconductivity in $AuTe_2$ when doped or under pressure.

One can phenomenologically describe this situation by an effective Hamiltonian like the Anderson lattice model (where $5p$ electrons of Te play the role of conduction electrons, while $5d$ electrons of Au are localized), but with an effective attraction—with negative U on localized levels. After excluding d electrons, we get in effect also an attraction of conduction electrons, which, on one hand, can provide the mechanism of CDW formation (not even requiring nesting of the Fermi surface, although nesting would help). And, on the other hand, in this model we have a natural mechanism of formation of Cooper pairs leading to superconductivity. In diagrammatic language, this mechanism of pairing is described in Fig. 4*B* [two electrons (or holes) of a conduction band "drop" into the Au $5d$ levels, where they experience attraction and form pairs, before decaying again into conduction electrons.] This situation is reminiscent of a model with bipolarons (36) and is different from the usual electron–phonon exchange in Fig. 4*A* (although the standard electron–phonon coupling could also contribute). Thus, $AuTe_2$ may be the long-sought second example of the same physics as proposed for $BaBiO_3$ (32), with the same mechanism of both charge disproportionation and superconductivity.

As Yet Unknown Compound AuTe

Since USPEX has shown its efficiency in determining the $AuTe_2$ crystal structure, we extended these calculations to a whole $Au_{1-x}Te_x$ series with arbitrary x. Fig. 5 shows thermodynamic convex hulls and a phase diagram of the Au–Te system in the GGA and GGA + SOC approximations. A compound is thermodynamically stable if its thermodynamic potential (e.g., the Gibbs free energy) is lower than that of any other phase or phase assemblage of the same composition. On a graph showing the enthalpy of formation of all compounds of a given system (e.g., Au–Te system) from the elements, all points corresponding to stable compounds can be connected to form a convex hull. Height above the convex hull is a measure of thermodynamic instability of a compound. One may note that in addition to experimentally observed structures such as $AuTe_2$ and $AuTe_3$ (37) there appears another one: AuTe.

AuTe has never been synthesized so far, but there exists mineral muthmannite, $AuAgTe_2$, found in Western Romania (38), where Au and Ag ions are in a 1:1 ratio. Muthmannite has a distorted NiAs-type structure with space group *P2/m*. Our calculations have shown that the *C2/c* structure predicted for AuTe by USPEX is significantly more stable (by 0.164 eV per atom with SOC) than the muthmannite structure. The predicted *C2/c* structure of AuTe, shown in Fig. 6, can be considered a distorted NaCl-type structure (NiAs and NaCl structures are relatives).

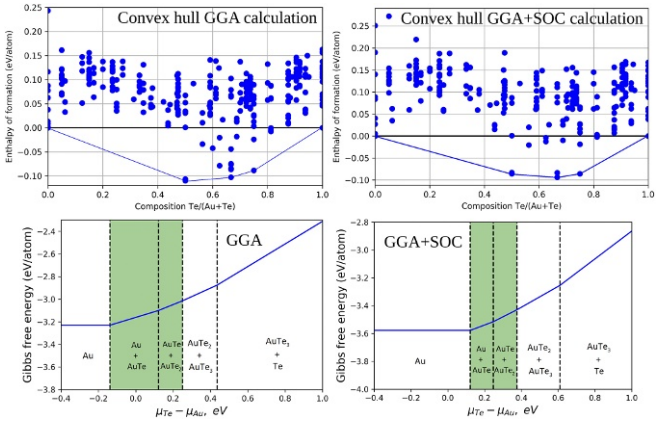

Fig. 5. Thermodynamic convex hulls and Gibbs free energy G vs. chemical potential μ for the Au–Te system with different Te concentrations.

The Au ions are in the strongly distorted plaquettes with two short (2.68 Å) and two long (2.90 Å) Au–Te bonds.

It is worthwhile mentioning that the SOC additionally lowers the position of the Au $5d$ band and thus affects stability of different phases in the Au–Te system. One can see from Fig. 5 that while both GGA and GGA + SOC calculations show stability of the same phases and crystal structures, there are large changes in stability fields. The plot of Gibbs free energy vs. chemical potential demonstrates that inclusion of the SOC expands the stability field of Au (in effect making it more inert) and $AuTe_2$, at the expense of shrinking the stability fields of AuTe and $AuTe_3$. The relatively narrow stability field may explain why AuTe is not yet known.

AuTe was found to be a nonmagnetic metal in the GGA + SOC calculations. Analysis of the charge density, $\rho(\vec{r})$, corresponding to the bands at the Fermi level, shows that there are nearly equal contributions to $\rho(\vec{r})$ from Au $5d$ and Te $5p$ states. This may explain why USPEX did not find the solution corresponding to charge disproportionation, as it did for calaverite (two inequivalent Au ions: in dumbbells and plaquettes): The energy costs due to the on-site Coulomb repulsion are too large in AuTe. Thus, in effect AuTe should resemble the high-pressure phase of $AuTe_2$, with all Au equivalent, and one could expect that it could also be superconducting.

Conclusions

The Au–Te system presents an interesting example of compounds of a very inert element, gold, with nontrivial properties. We found that there exist in the Au–Te system three stable stoichiometric compounds: AuTe, $AuTe_2$, and $AuTe_3$. [There exists also Au_3Te_7 with a simple cubic structure and statistical distribution of Au and Te atoms (39), but it is likely a solid solution. We have not found a stable compound with such stoichiometry in calculations at T = 0 K, which indicates that it is probably entirely entropy stabilized.] The second and the less "popular" third compound are known and studied. AuTe has not been synthesized, however, although a similar material, mineral muthmannite $AuAgTe_2$, is known. It would be very interesting to check our predictions and try to synthesize and study AuTe.

Much better studied, but still presenting several, until now unresolved puzzles, is calaverite, $AuTe_2$. This is the system whose properties we now explain on the basis of ab initio calculations. The picture emerging from our calculations is the following: The nominal average valence of gold in $AuTe_2$ is 2+, similar to many pyrites like FeS_2 and MnS_2 (40). But this state is, first of all, chemically unstable (only Au^{1+} and Au^{3+} are known to exist, with very few exceptions). And, most importantly, both Au^{2+} and Au^{3+} in $AuTe_2$ correspond to the situation with negative CT energy, that is, practically $Au^{2+} \rightarrow Au^{1+}\underline{L}$ and $Au^{3+} \rightarrow Au^{1+}\underline{L}^2$. This means that in fact all of the holes go to ligand (here Te) bands (but still with significant hybridization with d states of Au). This is actually the situation of self-doping (17, 19). In this case there occurs a phenomenon met also in several other systems: the valence, or charge disproportionation, which, however, again occurs not so much on the d shells themselves, but on ligands; that is, corresponding disproportionation is described not as in Eq. **1**, but instead as in Eq. **2**. This transition is accompanied (and is largely driven) by the change of the Au–Te bond lengths (and local coordination—linear for Au^{1+} and square for $Au^{3+} = Au^{1+}\underline{L}^2$); that is, it should be better called not charge, but bond disproportionation (17). But the outcome is very similar: There occurs in this case a structural transition with the formation of corresponding superstructures, commensurate as in, e.g., nickelates $RNiO_3$ (17, 22, 23) or incommensurate as in the case of a frustrated triangular lattice of $AuTe_2$. This picture naturally explains both the structural characteristics of $AuTe_2$ and the spectroscopic data, showing apparently constant occupation of d shells of Au. Despite this equivalence, the tendency to this charge or bond disproportionation is intrinsically connected with the "atomic" property of, here, Au (skipped valence Au^{2+}). Suppression of this superstructure by pressure or doping leads to the formation of a homogeneous metallic state with all Au (or Ni in $RNiO_3$) becoming equivalent, and in $AuTe_2$ this state becomes superconducting. The situation with negative CT gap and with a lot of ligand holes existing in particular in $AuTe_2$ is the solid state analogue of dative bonding known in coordination chemistry.

We argue that the same mechanism—the tendency to charge disproportionation, which is in fact the tendency to form electron or hole pairs—may be instrumental for the appearance of superconductivity in doped $AuTe_2$ or $AuTe_2$ under pressure. Thus, this exciting material, gold telluride, indeed is extremely interesting, both because of its rich history and, more important for us, as an example of very interesting physics.

Methods

The DFT calculations were performed within the Perdew–Burke–Ernzerhof functional (41) using the all-electron PAW method (42) as realized in the VASP code (43). We took into account the SOC and used scalar-relativistic GW PAW potentials with an [Xe] core (radius 2.1 a.u.) and [Kr] core (radius 2.2 a.u.) for Au and Te atoms, respectively, and plane wave cutoff of 400 eV. The evolutionary structure prediction algorithm USPEX (27) was applied in the search for stable phases. Structure relaxations used k-mesh with a resolution of $2\pi \times 0.03$ Å^{-1} and electronic smearing of 0.1 eV. The USPEX simulation included 80 structures per generation for a

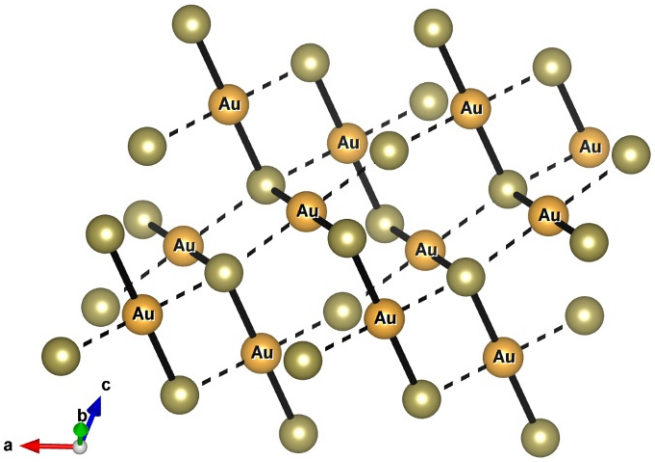

Fig. 6. The crystal structure of AuTe. Thick solid and dashed lines correspond to short and long Au–Te bonds, respectively.

variable-composition run. Also all known Au–Ag–Te compounds (with silver atoms substituted by gold) were included in the calculation (6, 37, 39, 44, 45). Phonon calculations were performed using Phonopy (31) with a $4 \times 4 \times 2$ supercell.

ACKNOWLEDGMENTS. We are grateful to G. Sawatzky, S.-W. Cheong, P. Becker, and L. Bohaty for discussions. This work was supported by the UralBranch of Russian Academy of Sciences (18-10-2-37), by the Russian Foundation of Basic Research (16-32-60070), by the Federal Agency of Scientific Organizations ("spin" AAAA-A18-118020290104-2), by the Russian Ministry of Science and High Education (02.A03.21.0006), by Russian President Council on Science (MD-916.2017.2), by the DFG (SFB 1238), and by the German Excellence Initiative. A.R.O. thanks the Russian Science Foundation (16-13-10459). V.V.R. was supported by Project 5-100 of Moscow Institute of Physics and Technology, and computations were performed on the Rurik supercomputer.

1. Dam B, Janner A, Donnay JDH (1985) Incommensurate morphology of calaverite $AuTe_2$ crystals. *Phys Rev Lett* 55:2301–2304.
2. Kitagawa S, et al. (2013) Pressure-induced superconductivity in mineral calaverite $AuTe_2$. *J Phys Soc Jpn* 82:113704.
3. Kudo K, et al. (2013) Superconductivity induced by breaking Te_2 dimers of $AuTe_2$. *J Phys Soc Jpn* 82:063704.
4. Ootsuki D, et al. (2014) Effect of Pt substitution on the electronic structure of $AuTe_2$. *Phys Rev B* 90:144515.
5. Reithmayer K, Steurer W, Schulz H, Boer DJ (1993) High-pressure single-crystal structure study on calaverite, $AuTe_2$. *Acta Crystallogr B Struct Sci* 49:6–11.
6. Tunell G, Pauling L (1952) The atomic arrangement and bonds of the gold-silver ditellurides. *Acta Crystallogr* 5:375–381.
7. Tendeloo GV, Gregoriades P, Amelinckx S (1983) Electron microscopy studies of modulated structures in (Au, Ag)Te_2: Part I. Calaverite $AuTe_2$. *J Solid State Chem* 50:321–334.
8. Krutzen BCH, Inglesfield JE (1999) First-principles electronic structure calculations for incommensurately modulated calaverite. *J Phys Condens Matter* 2:4829–4847.
9. Gonze X, Caracas R, Sonnet P, Detraux F (2000) First-principles study of crystals exhibiting an incommensurate phase transition. *AIP Conference Proceedings*, eds Cohen RE, Mewaldt RA (Am Inst Physics, College Park, MD), Vol 535, pp 163–172.
10. Schutte WJ, de Boer JL (1988) Valence fluctuations in the incommensurately modulated structure of calaverite $AuTe_2$. *Acta Crystallogr Sec B* 44:486–494.
11. Elder SH, Lucier GM, Hollander FJ, Bartlett N (1997) Synthesis of Au(II) fluoro complexes and their structural and magnetic properties. *J Am Chem Soc* 119: 1020–1026.
12. Varma CM (1988) Missing valence states, diamagnetic insulators, and superconductors. *Phys Rev Lett* 61:2713–2716.
13. Ushakov AV, Streltsov SV, Khomskii DI (2011) Crystal field splitting in correlated systems with negative charge-transfer gap. *J Phys Condens Matter* 23:445601.
14. van Triest A, Folkerts W, Haas C (1990) Electronic structure and photoelectron spectra of calaverite, $AuTe_2$. *J Phys Condens Matt* 2:8733–8740.
15. Ettema A, Stegink T, Haas C (1994) The valence of Au in $AuTe_2$ and AuSe studied by x-ray absorption spectroscopy. *Solid State Commun* 90:211–213.
16. Khomskii D (1997) Unusual valence, negative charge-transfer gaps and self-doping in transition-metal compounds. *Lithuanian J Phys* 37:65.
17. Sawatzky G, Green R (2016) The explicit role of anion states in high-valence metal oxides. *Quantum Materials: Experiments and Theory Modeling and Simulation*, ed Pavarini E (Verlag des Forschungszentrum, Jülich, Germany), Vol 6, pp 1–36.
18. Zaanen J, Sawatzky G, Allen J (1985) Band gaps and electronic structure of transition-metal compounds. *Phys Rev Lett* 55:418–421.
19. Korotin MA, Anisimov VI, Khomskii DI, Sawatzky GA (1998) CrO_2: A self-doped double exchange ferromagnet. *Phys Rev Lett* 80:4305–4308.
20. Goodenough JB (1963) *Magnetism and the Chemical Bond* (Interscience Publishers, New York).
21. Hoffmann R, et al. (2016) From widely accepted concepts in coordination chemistry to inverted ligand fields. *Chem Rev* 116:8173–8192.
22. Alonso JA, et al. (1999) Charge disproportionation in $RNiO_3$ perovskites: Simultaneous metal-insulator and structural transition in $YNiO_3$. *Phys Rev Lett* 82:3871–3874.
23. Mizokawa T, Khomskii DI, Sawatzky GA (2000) Spin and charge ordering in self-doped Mott insulators. *Phys Rev B* 61:11263–11266.
24. Bader RFW (1994) *Atoms in Molecules: A Quantum Theory*, *International Series of Monographs on Chemistry* (Clarendon, Oxford).
25. Rodriguez-Carvajal J, et al. (1998) Neutron-diffraction study of the Jahn-Teller transition in stoichiometric $LaMnO_3$. *Phys Rev B* 57:R3189–R3192.
26. Haegele VR, Babel D (1974) Die Neubestimmung der K_2CuF_4-struktur [Refinement of K_2CuF_4 structure]. *Z Anorg Allg Chem* 409:11–22. German.
27. Oganov AR, Glass CW (2006) Crystal structure prediction using ab initio evolutionary techniques: Principles and applications. *J Chem Phys* 124:244704.
28. Dong X, et al. (2017) A stable compound of helium and sodium at high pressure. *Nat Chem* 9:440–445.
29. Zhang W, et al. (2013) Unexpected stable stoichiometries of sodium chlorides. *Science* 342:1502–1505.
30. Zhang J, et al. (2015) Pressure-induced novel compounds in the Hf-O system from first-principles calculations. *Phys Rev B* 92:184104.
31. Togo A, Tanaka I (2015) First principles phonon calculations in materials science. *Scr Mater* 108:1–5.
32. Rice T, Sneddon L (1981) Real-space and k-space electron pairing in $BaPb_1$-$xBixO_3$. *Phys Rev Lett* 47:689–692.
33. Khomskii DI, Zvezdin AK (1988) "Neutral oxygen" and superconductivity of metalloxide systems. *Solid State Commun* 66:651–655.
34. Robaszkiewicz S, Micnas R, Ranninger J (1987) Superconductivity in the generalized periodic Anderson model with strong local attraction. *Phys Rev B* 36:180–201.
35. Friedberg R, Lee TD (1989) Gap energy and long-range order in the boson-fermion model of superconductivity. *Phys Rev B* 40:6745–6762.
36. Micnas R, Ranninger J, Robaszkiewicz S (1990) Superconductivity in narrow-band systems with local nonretarded attractive interactions. *Rev Mod Phys* 62:113–171.
37. Luo HL, Merriam MF, Hamilton DC (1964) Superconducting metastable compounds. *Science* 145:581–583.
38. Bindi L, Cipriani C (2004) Ordered distribution of Au and Ag in the crystal structure of muthmannite, $AuAgTe_2$, a rare telluride from Sacarîmb, western Romania. *Am Mineral* 89:1505–1509.
39. Newkirk L, Tsuei C (1971) Superconducting transition temperatures and lattice parameters of simple-cubic metastable Te-Au solutions containing Fe and Mn. *Phys Rev B* 3:755.
40. Wilson JA, Yoffe AD (1969) The transition metal dichalcogenides discussion and interpretation of the observed optical, electrical and structural properties. *Adv Phys* 18:193–335.
41. Perdew JP, Burke K, Ernzerhof M (1996) Generalized gradient approximation made simple. *Phys Rev Lett* 77:3865–3868.
42. Blöchl PE (1994) Projector augmented-wave method. *Phys Rev B* 50:17953.
43. Kresse G, Furthmüller J (1996) Efficient iterative schemes for ab initio total-energy calculations using a plane-wave basis set. *Phys Rev B* 54:11169.
44. Belov N, Spiridonov E, Chamid S, Pobedimskaya E (1978) Refinement of the structure of petzite $AuAg_3Te_2$. *Kristallografiya* 23:483–486.
45. Bachechi F (1971) Crystal structure of Montbrayite locality: Robb-Montbray, Quebec. *Nat Phys Sci* 231:67–68.